Biophysical Journal Volume 107 July 2014 355–364

Article

Self-Assembly of Polysaccharides Gives Rise to Distinct Mechanical Signatures in Marine Gels

G. Pletikapić,[1] H. Lannon,[3] Ü. Murvai,[2] M. S. Z. Kellermayer,[2] V. Svetličić,[1] and J. Brujic[3,*]

[1]Division for Marine and Environmental Research, Ruđer Bošković Institute, Zagreb, Croatia; [2]Department of Biophysics and Radiation Biology, Semmelweis University, Budapest, Hungary; and [3]Center for Soft Matter Research and Department of Physics, New York University, New York, New York

ABSTRACT Marine-gel biopolymers were recently visualized at the molecular level using atomic force microscopy (AFM) to reveal fine fibril-forming networks with low to high degrees of cross-linking. In this work, we use force spectroscopy to quantify the intra- and intermolecular forces within the marine-gel network. Combining force measurements, AFM imaging, and the known chemical composition of marine gels allows us to identify the microscopic origins of distinct mechanical responses. At the single-fibril level, we uncover force-extension curves that resemble those of individual polysaccharide fibrils. They exhibit entropic elasticity followed by extensions associated with chair-to-boat transitions specific to the type of polysaccharide at high forces. Surprisingly, a low degree of cross-linking leads to sawtooth patterns that we attribute to the unraveling of polysaccharide entanglements. At a high degree of cross-linking, we observe force plateaus that arise from unzipping, as well as unwinding, of helical bundles. Finally, the complex 3D network structure gives rise to force staircases of increasing height that correspond to the hierarchical peeling of fibrils away from the junction zones. In addition, we show that these diverse mechanical responses also arise in reconstituted polysaccharide gels, which highlights their dominant role in the mechanical architecture of marine gels.

INTRODUCTION

Marine gels consist of three-dimensional networks of solvated biopolymers embedded in seawater. The importance of the gel phase in marine ecosystems has been widely recognized among scientists from different fields due to their role in the microbial loop and sedimentation processes, biogeochemical carbon cycling, marine carbohydrate chemistry, and particle dynamics in the ocean (1–5). Marine gels exhibit a wide range of polydispersities, ranging from microscopic to macroscopic dimensions up to giant gel macroaggregates in the Northern Adriatic (6–8). These gels, which are bioreactive, are important because they compartmentalize nutrients and thus enhance microbial activity (9,10). Their 3D structure, obtained by cryo-scanning electron microscopy (cryo-SEM) (11) and by atomic force microscopy (AFM) (12), consists of a small amount of organic matter that swells to hold a large volume of water within its reactant pockets. The mechanical hierarchy within the gel structure could serve to provide a safe haven for microorganisms and therefore increase their adaptability to the external environment.

Gel formation in aqueous solutions, such as seawater, is a complex process that depends on the biopolymer's chemical structure, nature of co- and counter ions, polymer concentration, and temperature. Microscopic (transmission electron microscopy and AFM) and NMR studies reveal that fibrillar acyl heteropolysaccharides are the major constituents of naturally occurring marine high-molecular-weight dissolved organic matter (13,14). These polysaccharides form porous self-assembled microgels throughout the water column ((5) and references therein). They are produced by marine phytoplankton and are composed of repeating units of several types of monosaccharides (including galactose, glucose, fucose, mannose, and xylose) in conjunction with glycosidic bonds (15). The natural gel material used in this study was collected in the northern Adriatic Sea during an episode of massive gel formation, known as a mucilage event. The most comprehensive chemical characterization of gel macroaggregates from this aquatorium shows that carbohydrates are the principal organic fraction and that the average ratio of polysaccharide to total organic carbon is 41.5% (16). More specifically, gas-chromatographic analysis of purified polysaccharides yields a set of six neutral monosaccharides: galactose (35%), glucose (16%), mannose (11%), xylose (9.5%), rhaminose, fucose, and other, minor constituents. These are polydisperse heteropolysaccharides in which some of the hydroxyl groups of sugar residues are substituted by ester sulfate groups and, to a minor extent, carboxylic groups (17). More labile polysaccharides primarily consist of α-glucosidic bonds, whereas those in the gel matrix mainly consist of β-glucosidic bonds (18). The greater stability of β-glucosidic bonds explains why the gels are difficult to break down (19). Since monosaccharide compositions of

Submitted February 11, 2014, and accepted for publication April 28, 2014.

*Correspondence: jb2929@nyu.edu

Editor: Margaret Gardel.

0006-3495/14/07/0355/10 $2.00

http://dx.doi.org/10.1016/j.bpj.2014.04.065

self-assembled marine gels are similar throughout the oceans, the results presented here are universal to all marine-gel networks formed by self-assembly.

Apart from the polysaccharide content, marine gels also contain a smaller fraction of lipids, proteins, and nanoparticles, which renders their analysis complex. Exopolysaccharides released by the diatom *Cylindrotheca closterium* under conditions of increased production (20) comprise a simpler system that has the same chemical composition of polysaccharides as marine gels. In addition, their polymer networks have the same features—fibril heights, pore openings, and mode of fibril association—as native gel samples from the Northern Adriatic (21). Given these similarities, we compare here the mechanical and structural properties of complex natural gel samples with those of the simplified system of reconstituted polysaccharides released by the diatom *C. closterium*. This comparison allows us to expose the role of heteropolysaccharides in the marine-gel structure and mechanical response. These polysaccharides exhibit supramolecular organization and gelation due to hydrogen bonding and electrostatic interactions (22). Unlike chemically cross-linked gels, polysaccharide electrolytes form gels by physical intermolecular bonds between polymer chains (23–25). Indeed, AFM imaging and differential scanning calorimetry confirm that the marine gel is a thermoreversible physical gel (12). The observed microstructure reveals monomolecular, helical, and superhelical associations within the gel, which are characteristic of the cross-linking of polysaccharide fibrils by hydrogen bonding. Alternative gelation mechanisms proposed include bridging between biopolymers by Ca^{2+} ions (26), hydrophobic interactions (27), and physical nucleation seeded by nanoparticles (11). Due to the inherent complexity and heterogeneity of the system, it is difficult to isolate the physical forces within the marine biopolymer networks.

From a structural perspective, the isolated and purified polysaccharides at concentrations >10 mg/L are known to form chain associations or multiple helical structures (8). These polysaccharides have a larger radius of gyration and larger stiffness parameters than either the flexible chains of pullulan or the semirigid chains of the bacterial polysaccharides wellan and alginate (22). It remains an open question how these associations influence the mechanical properties of the gel. Studying the mechanics of marine gels broadly impacts our understanding of hierarchical biopolymer networks such as those found in the extracellular matrix of bacteria (28) or the adhesive proteoglycans in marine sponges (29).

In this study, we control the degree of gel-network entanglements by dilution and stirring to study single fibrils and their associations. The techniques we use are force spectroscopy and high-resolution AFM imaging, which allow us to investigate the relationship between the marine biopolymer morphology and its nanomechanical response to external pulling force. The native marine gels are constantly exposed to mechanical perturbations caused by local hydrodynamics (turbulence and shear) as well as large-scale physical processes (strong winds and currents), rendering the application of hundreds of piconewtons of force highly biologically relevant. By investigating the gel network at different degrees of association, we probe the microscopic structures within each assembly. Interestingly, we discover four distinct mechanical responses at different levels of fibril association. All the features present in the complex marine-gel system are also found in the marine-gel polysaccharide fraction, confirming the existence of similar mechanical hierarchies within both networks.

MATERIALS AND METHODS

The marine-gel material used in this study was collected at the off-shore station in the Northern Adriatic SJ 107 (45°02.8'N, 13°19.0'E) in the summer of 2010 (sampling date August 18, 2010, depth 15 m) during a regular cruise along the transect between the Po River Delta and Rovinj, on the Istrian coast. Marine gels are usually dispersed as micro- or nanoparticles in the ocean (30), which makes sampling, handling, and concentrating the sample a challenging task. The massive formation of gelatinous macroaggregates in the northern Adriatic Sea offered a consistent source of concentrated gel material and the possibility for systematic structural studies. The polysaccharide fractions, either from marine-gel samples or from the axenic *C. closterium* culture medium, were isolated according to the procedure described in Urbani et al. (20) and Zoppini et al. (31). Dr. Urbani, of the Faculty of Sciences, University of Trieste, provided us with isolated and purified polysaccharide fractions (see Supporting Material).

AFM imaging

AFM imaging was performed using a Multimode AFM with NanoScope IIIa controller (Veeco Instruments, Santa Barbara, CA) with a vertical-engagement JV 125 mm scanner. The tapping mode was applied using silicon tips (RTESP, Veeco, resonance frequency 289–335 kHz, spring constant in the range 20–80 N/m). The set-point/free amplitude ratio (A/A_0) was maintained at 0.9 (light tapping). The linear scanning rate was optimized between 1.0 and 1.5 Hz with scan resolution of 512 samples/line. Processing and analysis of images was carried out using NanoScope software (version V614r1, Digital Instruments, Buffalo, NY). All images presented are raw data except for the first-order two-dimensional flattening. Samples were prepared using the drop-deposition method modified for marine samples (12,21,32,33) and imaged in air (see Supporting Material). Each specimen was examined by imaging 5–10 randomly chosen positions with scanned areas from 50 × 50 μm down to 1 × 1 μm. The imaged networks shared the same features in terms of fibril height, pore opening, and mode of fibril association (12).

Force spectroscopy

The MFP3D force spectrometer (Asylum Research, Santa Barbara, CA) was used in preliminary experiments on marine gel samples to obtain a general appearance of force curves at 10 μm extension. To study specific patterns on force extension curves, we used a custom-built AFM apparatus consisting of a modified Digital Instruments detector head (AFM-689, Veeco Instruments) and a three-dimensional piezoelectric translator with a range of 5 μm and a resonant frequency of ~10 kHz (P-363.3CD, Physik Instrumente, Karlsruhe, Germany). Laser position and alignment were performed using a photodiode at 100 kHz (Schäfter & Kirchhoff, Hamburg,

Germany). Silicon nitride cantilevers (MLCT, Bruker Probes, Camarillo, CA) were used, with spring constants calibrated to be 10–50 pN/nm using the equipartition theorem. All experiments were performed at room temperature. The experiment was regulated by a proportional-integral-derivative controller and run using software written in Igor PRO.

Marine-gel phase was first dispersed in filtered seawater (0.2 μm filter, salinity 37.2, pH 8.2, dissolved organic carbon 100 μM). Generally, 0.4 cm^3 of gel phase was dispersed in 80 mL of seawater (gel volume fraction, $\phi_G \sim 0.5\%$). Fifty-microliter aliquots of the suspension were pipetted onto the glass substrate and left for 2 h while polymers adsorbed to the surface. Filtered seawater was used as a force spectroscopy buffer. Force curves were collected at different levels of entanglement. The level of entanglement was controlled by duration of stirring (2, 4, and 24 h) to obtain force curves with the optimal number of stretching and/or unfolding events. The nanomechanical response of the marine gel at low salinity was recorded in seawater diluted by ultrapure water 1:8. Solutions containing 10–40 mg/L of isolated polysaccharide fractions were also prepared in filtered seawater. To pick up a biopolymer, the AFM tip was pressed down onto the sample for 1–3 s at forces of 0.8–15 nN. The coupling of the marine biopolymers to the tip was based on a nonspecific interaction. In the case of disentangled polysaccharides, the AFM tip was pressed down onto the sample for 3 s at intentionally higher force values (from 5 nN up to 15 nN) to ensure stronger coupling of the biopolymers to the tip. This protocol allowed us to observe the shoulder-like transitions that typically occur at high forces (>400 pN).

In total, we collected several thousand force curves for partially disintegrated marine-gel networks and for isolated polysaccharides with a similar degree of cross-linking. We identified reproducible patterns in force-extension curves that were categorized into four types: 1), individual nonlinear peaks; 2), sawtooth patterns; 3), force plateaus; and 4), force steps. To quantify the elastic response of individual fibrils we used the wormlike chain (WLC) model (34,35). Individual nonlinear peaks that showed significant deviations from the model were not taken into account. For the analysis of sawtooth peaks, we included only patterns containing three or more repetitive peaks with a gradually increasing or steady force, defined by a sharp relaxation to the baseline, and we allowed for a minimal drift of only 10% in the force. Irregular sawtooth patterns were disregarded to avoid spurious interactions. The frequency of accepted trajectories in a typical experiment was ~10% and was lower for isolated polysaccharides due to the low probability of picking up a single chain.

To identify the force plateaus and staircases, we accepted flat regions of constant force that are longer than 25 nm. Trajectories with larger drift were excluded from the analysis (for more details, see Supporting Material). The frequency of force steps in a successful experiment was ~5–20% for marine gels dispersed in diluted seawater and <5% for those in seawater.

RESULTS AND DISCUSSION

Marine-gel networks at varying degrees of polymer association

It was recently proposed that marine gels are thermoreversible physical gels comprised of cross-linked polysaccharide fibrils, which form higher-order structures mainly via hydrogen bonding (17). In Fig. 1 *A*, we show the network structure of a native marine gel diluted 100 times in seawater, visualized by high-resolution AFM imaging. Further dilution and stirring disintegrates the network to lower degrees of cross-linking (Fig. 1 *B*) or to isolated single fibrils (Fig. 1 *C*). In a similar way, polysaccharide fibrils from the extracellular polymeric substance (EPS) of diatoms (Fig. 1 *D*) or from the native gel (Fig. 1 *E*) assemble into a gel network structure from the single fibrils shown in Fig. 1 *F* (8,21,22). A quantitative analysis of similar AFM images has recently been interpreted in terms of the molecular organization of the gel network, such as the associations between the polysaccharide fibrils therein (12).

Here, we gain further insight into the molecular organization of the marine and polysaccharide gels by force spectroscopy. To correlate nanomechanical responses of fibrils to an external pulling force with the topology of the fibrils on the nanoscale, we performed both force spectroscopy and AFM imaging on the same gel suspension. In both cases, we control the gel network state by different conditions of dilution and stirring. The level of entanglement

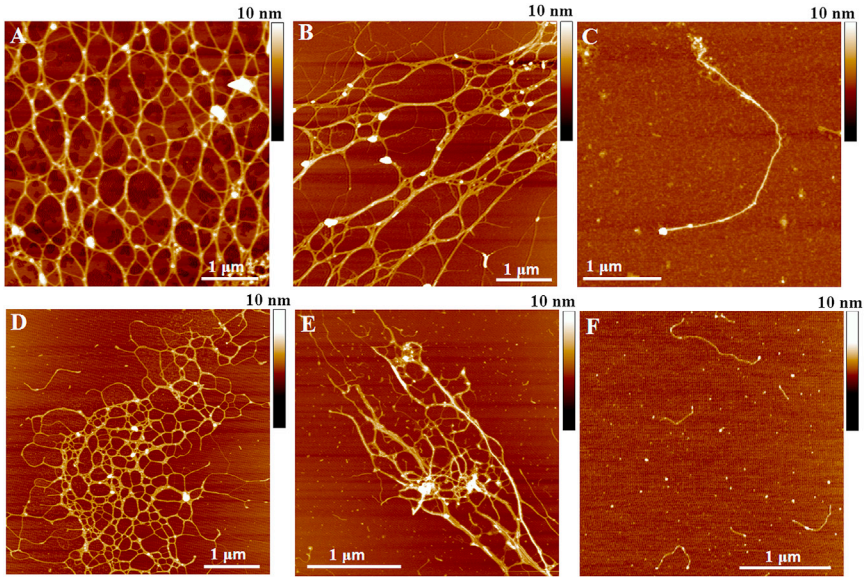

FIGURE 1 AFM images of native marine gel (*A–C*) and polysaccharides isolated from *C. closterium* EPS (*D*) and from native marine gel (*E*) at different levels of association. (*A–C*) Levels of entanglement were $\phi \sim 1\%$, with 4 h stirring (*A*), $\phi_G \sim 0.5\%$, with 4 h stirring (*B*), and $\phi_G \sim 0.5\%$, with 24 h stirring (*C*). Concentrations of purified polysaccharides were 20 mg/L, with 2 h stirring (*D* and *E*). (*F*) Single fibrils of polysaccharides isolated from *C. closterium* EPS, 10 mg/L concentration and 2 h stirring. To see this figure in color, go online.

was controlled by the duration of stirring (2, 4, and 24 h), which led to distinct force curves with reproducible features in the stretching and/or unfolding events.

Disentangled networks give rise to entropic elasticity

In the most dilute case, we pull on individual marine and polysaccharide fibrils and obtain force-extension curves that are well fit by the WLC model (Fig. 2, *A* and *B*). This result indicates a purely entropic response to the stretching force. Nevertheless, we find different persistence lengths (Lp) of the fibrils, spanning a broad range of 0.2–4 nm, although more than half of these lengths are <1 nm. Since the WLC model has two parameters in the fit, we obtain Lp and contour length simultaneously for each individual peak.

This result is corroborated by the image in Fig. 2 *C*, which shows fibrils of different stiffness. AFM imaging was performed to check whether individual fibrils are present in the sample and to measure the heterogeneity of their heights. This height can roughly be correlated to the number of associated monomolecular fibrils, which in turn affects fibril stiffness. For example, in our sample, we detected fibrils with heights ranging from 0.6 to 2.6 nm, which corresponds to around four fibril associations. This result can therefore account for the persistence length range of 0.2–0.8 nm, which is where the majority of the data lie. Two fibrils with different heights are shown in Fig. 2 *C*.

The diversity in persistence length may arise from the assembly of several monomolecular fibrils into one bundle, as shown by the height difference between the individual fibrils in the image. Stretching multiple fibrils coupled in parallel reduces the apparent persistence length according to Lp/n, where n is the number of individuals in the bundle (36). Moreover, the heterogeneous chemical composition of the fibrils also leads to a difference in their flexibility (17). Values of Lp obtained here are greater than those of flexible biopolymers on a bacterial surface (Lp = 0.154–0.2 nm (37)), but comparable to polymers on a diatom surface (Lp = 1.8 nm (38)). In addition, the contour length of stretched fibrils exhibits a broad distribution and spans the entire 2 μm extension range of the AFM. These results are in agreement with fibril lengths of polysaccharides isolated from marine gels in the range 0.1–2 μm, as measured by dynamic light scattering (8).

Single-fibril extension reveals molecular polysaccharide transitions

In some cases of single-fibril pulls, the WLC model is followed by an additional extension, which manifests as a shoulder in the force-extension curves. Such mechanical behavior is very heterogeneous in the marine gels and gives rise to a broad, perhaps continuous, distribution of shoulder-like mechanical responses (data not shown). However, normalizing the end-to-end length at the shoulder value of the force and filtering the broad distribution that includes all the data in the polysaccharide system reveals a subset of data featuring three reproducible populations with distinct molecular signatures (Fig. 3, *A–C*). Since the fibrils have varying lengths, we normalize each trajectory by the value of the end-to-end length at 400 pN, which approximately corresponds to the value of the force at the shoulder. The superimposed segments with shoulders resemble those observed in chair-to-boat transitions of single-molecule polysaccharides (39–42). Above a threshold force, each monomer in the chain crosses a transition-state barrier to reach the extended boat conformation, which gives rise to a smooth extension in length. Therefore, we infer that the polysaccharide fibrils in the marine gel also exhibit such molecular transitions. The difference between the three profiles in Fig. 3 may arise due to distinct linkages between monomers within each polysaccharide chain. For example, α-1,4 linkages in amylose give trajectories with a profile similar to that seen in Fig. 3 *C*, whereas dextran exhibits a more pronounced extension at higher forces (40). A study on the underivatized oligosaccharide composition of the water-soluble fraction of marine gels by liquid chromatography, coupled to electrospray tandem mass spectrometry (43), revealed the presence of α-Glc-(1–4)$_n$ maltodextrins for macroaggregates collected in various locations of the northern Adriatic Sea. The presence of α or β 1–3 glycosidic bonds was also suggested. The diversity and complexity of linkages between individual monosaccharidic units in high-molecular-weight organic polymers (14) is expected to give a very broad variation in the force shoulder length and shape. The fact that 20% of trajectories revealed

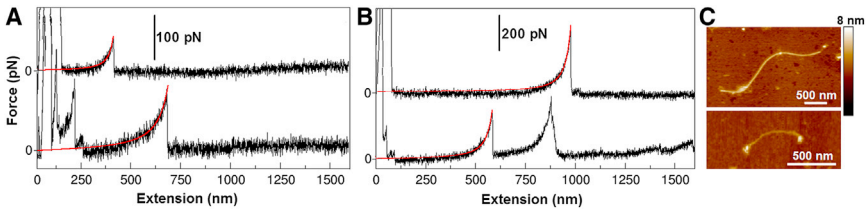

FIGURE 2 (*A* and *B*) Simple force-extension curves with one or a few individual peaks are shown for the marine gel (*A*) and for polysaccharides isolated from the marine gel (*B*). Individual peaks are fitted with the WLC model (*red lines*). (*C*) AFM image revealing the presence of fibrils of varying height (~2.2 nm and ~1.3 nm) and length (~3 μm and ~700 nm). Native marine gels are dispersed in seawater ($\phi_G \sim 0.5\%$) and stirred for 24 h. Polysaccharides isolated from marine gels are dissolved in seawater to a concentration of 10 mg/L and stirred for 2 h. To see this figure in color, go online.

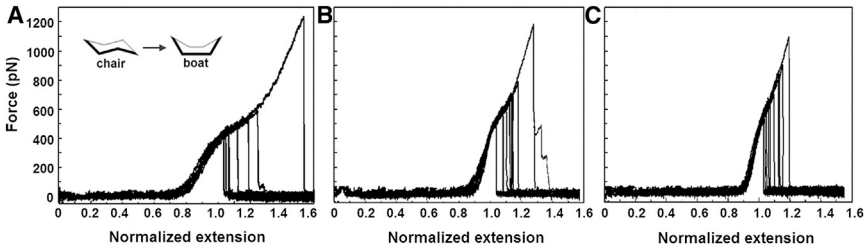

FIGURE 3 Superimposed normalized peaks with characteristic shoulders obtained by pulling isolated polysaccharides from the *C. closterium* EPS. Polysaccharides are dissolved in seawater to a concentration of 10 mg/L and stirred for 2 h.

superimposable patterns (by eye) after normalization is indicative of molecular transitions, such as specific chair-to-boat transitions, which are particularly abundant in our sample. Although we cannot pinpoint which monosaccharide fraction corresponds to each response at this stage, we display the statistical distribution of reproducible responses within such a complex system.

Partially disentangled networks reveal sawtooth patterns

In marine-gel samples with higher levels of fibril entanglement ($\phi_G \sim 0.5\%$, 2–4 h stirring), we obtain strikingly long force-extension trajectories extending beyond 8 μm (Fig. 4). These trajectories exhibit long regions with no mechanical resilience followed by clusters of sharp force peaks. We isolated distinct regions of multiple peaks (Fig. 5, *A* and *B*) for the marine and polysaccharide gels, respectively (additional examples are presented in Fig. S1, *A–D*, in the Supporting Material). Such repetitive sawtooth patterns in force spectra arise when the apparent contour length of the manipulated molecular system increases in discrete events. Indeed, the histograms of rupture forces (Fig. S1 *E*) and peak-to-peak distances (Fig. 5 *C*) reveal a periodicity in the underlying structure, with the most probable extensions in the narrow range of 10–20 nm. Microscopically, these sawtooth patterns may arise from unraveling of the entangled globular structures, as shown in Fig. 5 *D*. Typically, such force curves are observed in the unfolding of modular proteins such as the Ig domains in titin (44) and tandem ubiquitins (see, e.g., Carrion-Vazquez et al. (45)) or modular proteins in diatom adhesive pads (46,47). In addition, similar multipeaks with rupture forces and distances between peaks of the same order were reported for breaking intermolecular bonds between adhesion proteoglycans isolated from marine sponges (29).

Given that these sawtooth patterns occur both in the marine and the isolated polysaccharide gels, they are likely to arise from evenly spaced polysaccharide entanglements rather than protein constituents. We postulate that these globules are present in the source material (photosynthetically produced polysaccharides), which suggests that they have a biologically relevant function. The molecular origin of the mechanical stability of the globules could reside in the hydrophobic interactions between specific polysaccharide segments (25).

Unzipping fibril associations results in force plateaus

In addition to sawtooth patterns, we also observe plateaus in the force spectra (Fig. 6, *A–C*; additional examples can be seen in Fig. S2). These plateaus are commonly attributed to the unzipping of a given structure (48), i.e., the successive rupture of serially-linked bonds of the same type that hold the structure together. The force remains constant because only one bond is loaded at a time. Although these plateaus are present in the marine as well as the polysaccharide gels, they are more frequent in the latter case. Marine-gel and polysaccharide force plateaus exhibit the distributions shown in Fig. 6 *D*. The plateau-force histogram for polysaccharides displays a lower peak value than does that for marine gels (200 vs. 300 pN), but its distribution is wider (50–800 vs. 50–450 pN). Both samples exhibit a similarly broad range of released lengths, 25–400 nm. Similar plateaus were observed in the force-extension of carrageenan

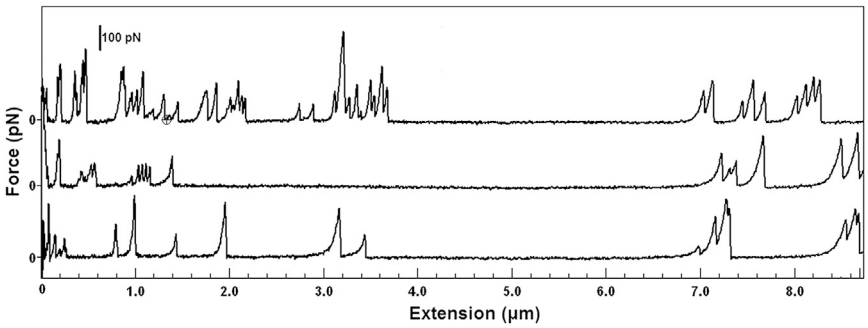

FIGURE 4 Long force-extension trajectories with individual peaks and more complex sawtooth patterns obtained by pulling a partially disintegrated marine gel. Native marine gel is dispersed in seawater ($\phi_G \sim 0.5\%$) and stirred for 4 h.

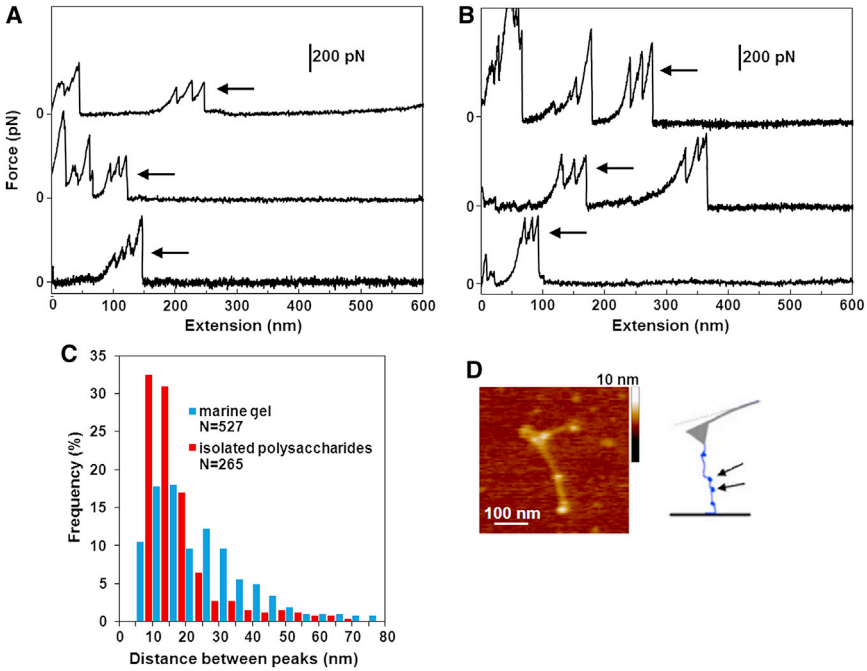

FIGURE 5 (*A* and *B*) Typical multipeak regions (*arrows*) are shown for the marine gel (*A*) and the marine-gel polysaccharides (*B*). (*C*) The distribution of distances between repetitive peaks for the marine gel and the marine-gel polysaccharides. (*D*) AFM image showing globular polysaccharide entanglements along an individual marine-gel fibril. The height of the globules (~2–2.5 nm) is twice that of the fibril (~1–1.5 nm). The schematic diagram shows the entanglements pulled by the AFM tip. Native marine gel is dispersed in seawater (ϕ_G ~ 0.5%) and stirred for 4 h. Polysaccharides isolated from marine gel are dissolved in seawater to a concentration of 20–40 mg/L and stirred for 4 h. To see this figure in color, go online.

(300 pN (49)), xanthan (400 pN (50,51)), and curdlan (60 pN (52)). These plateaus are attributed to the unzipping of double-stranded helices in the case of carrageenan and xanthan and triple-stranded helices in the case of curdlan. We therefore infer that our plateaus occur as a result of similar intermolecular associations. The diversity in the force-plateau values corresponds to the unzipping (as well as unwinding) of helices that involve multiple chains. This mechanism is in agreement with our previous work, which shows that up to six monomolecular fibrils associate into a single fibril within marine gels (12,21). In addition, we observe intertwined fibrils shown by AFM (Fig. 6 *E*), and these unzip according to the schematic diagram. These force-spectroscopy results confirm that the fibrils are hydrogen-bonded helical structures.

Hierarchical force staircases as a mechanical signature of the gel network

At the highest level of entanglement (ϕ_G ~ 0.5%, 2 h stirring), we sometimes observe a different mechanical response, which is a succession of high-to-low force staircases (Fig. 7 *A*). To study their microscopic origin, we test the effect of ionic strength on the mechanical response of the marine gel. Reducing the salinity of seawater leads to more frequent staircases with more steps that are longer in

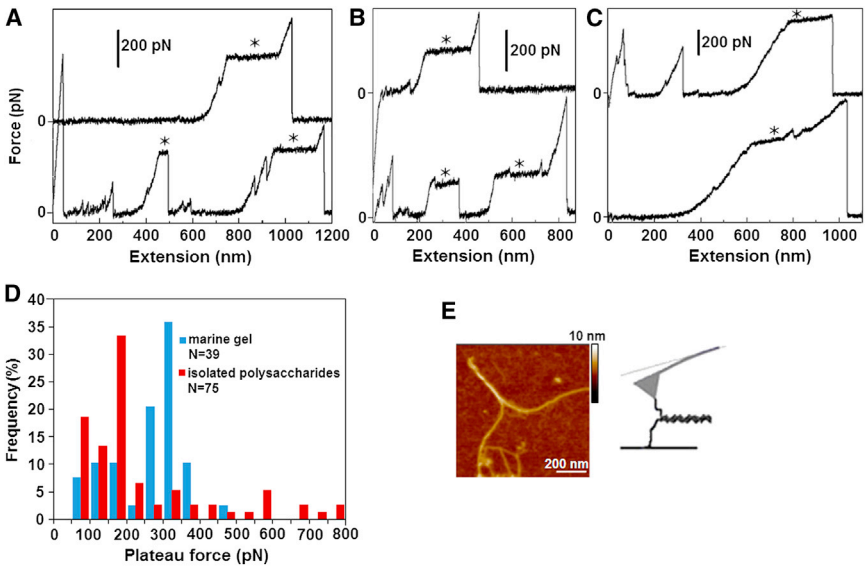

FIGURE 6 (*A–C*) Typical plateaus (*asterisks*) are shown for the marine gel (*A*) and the marine-gel polysaccharides (*B* and *C*). (*D*) Distribution of plateau forces for marine-gel biopolymers and isolated polysaccharides. An AFM image of an intertwined fibril is shown with a schematic representation of the unzipping of two chains. Native marine gel is dispersed in seawater (ϕ_G ~ 0.5%) and stirred for 4 h. Polysaccharides isolated from marine gel are dissolved in seawater to a concentration of 20–40 mg/L and stirred for 4 h. To see this figure in color, go online.

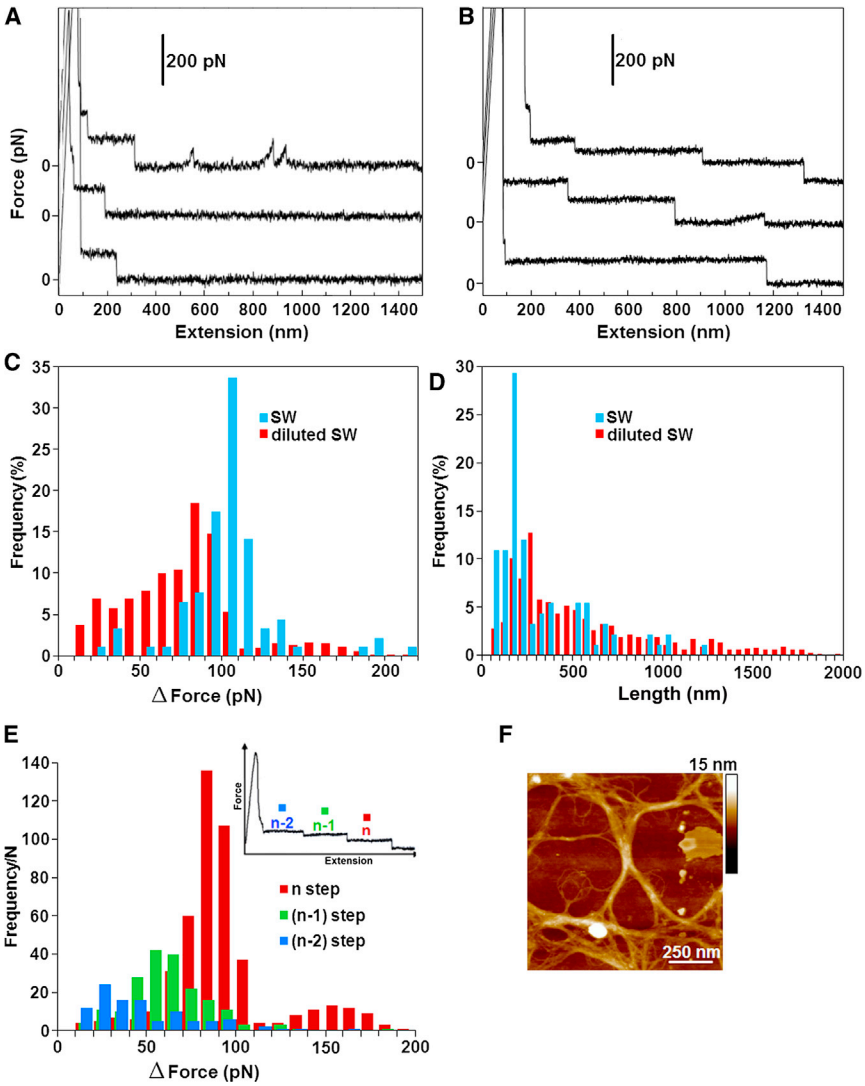

FIGURE 7 (*A* and *B*) Typical force staircases are shown for a marine gel in seawater (*A*) and in diluted seawater (*B*). (*C* and *D*) Step-force (*C*) and step-length (*D*) distributions. (E) Step-force distribution ranked by the reverse-order number of the step in the staircase. The AFM image shows junction zones that form the gel network. The native marine gel is dispersed in diluted seawater ($\phi_G \sim 0.5\%$) and stirred for 2 h.

length (Fig. 7 *B*). In total, we collect ~400 staircases, spanning from 1 to 11 steps down to the baseline of zero force. The distribution of the force difference between consecutive steps, ΔF, shows that the peak step size decreases from 110 to 80 pN upon dilution of seawater (Fig. 7 *C*). On the other hand, the peak step length increases from 150 to 250 nm (Fig. 7 *D*). In both cases, ranking the data by the reverse order number of the step, where the first step is the last in the staircase, reveals that the drop in force, ΔF, decreases with the rank for the diluted seawater gel (Fig. 7 *E*). Therefore, the last step in the staircase corresponds to the largest drop in the force. This result is consistent with the geometric interaction model derived to explain similar staircases observed in the case of carboxymethylcellulose (53). Their model proposes that the hierarchy arises from the consecutive peeling of individual fibrils away from a single linear bundle in a poor solvent.

Here, we propose an alternative origin for the hierarchical nature of the force staircases. These staircases reflect fibrils that are peeling away from the junction zones in the 3D gel network, rather than single linear bundles. These fibrils are embedded in branched structures interwoven into the gel fabric, as shown in Fig. 7 *F* for the diluted-seawater marine gel. As the fibril is being stretched, it liberates the junction zones within the network in order of their mechanical strength. The mechanical hierarchy arises because the highest-order junctions are released last and correspond to the largest drop in force. Interestingly, there is a bimodal distribution for the drop in force associated with the last step (Fig. 7 *E*). The smaller population consisting of 8% of trajectories exhibits a peak at 150 pN, which is approximately twice the value of the maximal peak (~80–90 pN). This could be due to the simultaneous peeling of fibrils away from two distinct junction zones within the gel network. Further evidence for fibril peeling comes from the AFM image, which shows that the lengths of the junction zones are in good agreement with the distribution of observed step lengths (Fig. 7 *D*). Our results are analogous to the

peeling of amyloid protofilaments away from the bundles by dismantling side-by-side associations (see, e.g., Kellermayer and colleagues (54–56)), but in our case, the fibrils are embedded in a gel matrix with junction zones of varying strengths. Note that long force steps can arise due to desorption of fibrils from the substrate in a train conformation (see, e.g., (57–61)). However, in our case, force staircases generally appeared at the highest level of entanglement ($\phi_G \sim 0.5\%$, 2 h stirring), and they were not detected in samples with disentangled fibrils, supporting the interpretation that they arise from unzipping of the gel network structure. Furthermore, if the force staircases did reflect desorption of fibrils from the surface, one would not expect the mechanical hierarchy shown in Fig. 7. Instead, the pulling of individual fibrils away from the surface in a train conformation would result in a uniform distribution of force steps, which is not the case in our data.

Moreover, the shorter step lengths measured in seawater are due to the decreased repulsion between polyelectrolytes, which gives rise to a more compact network with shorter junction zones. The mechanical hierarchy arises because the highest-order junctions are released last and correspond to the largest drop in force. It makes sense that the gel in seawater exhibits larger force steps, because the increased ionic strength leads to a higher degree of association between the polyelectrolyte chains, i.e., more multimeric chains (8). In particular, the average chain dimension as expressed by the radius of gyration, the weighted-average molecular weight (Mw), the second virial coefficient (A2), and the stiffness parameter (B) attests to the propensity of the polymer system to give elongated and stiff chains. Polysaccharides showed a marked polyelectrolytic behavior and intrinsic chain stiffness, favoring chain-to-chain association and/or gel formation at higher salt concentrations. For example, dynamic light scattering measurements reveal that polymers undergo an extensive degree of aggregation at higher salt concentrations (0.3–0.7 M) as a consequence of the screening effect of polymer charges.

CONCLUSIONS

This study shows that even though marine biopolymers are complex naturally occurring materials, careful experimentation using high-resolution AFM imaging and force spectroscopy can reveal reproducible and distinct mechanical responses. These mechanical signatures depend on the level of association between the fibrils and the topology of the gel network itself. Stretching individual fibrils or several fibrils associated into a single bundle is well captured by the WLC model for entropic elasticity with different persistence lengths. Further stretching of individual fibrils reveals conformational changes, such as the known chair-to-boat transition, within the polysaccharide chain. Interestingly, we uncover three distinct conformational extensions in the reconstituted gel obtained from the polysaccharide fraction of the marine diatom EPS. Although their exact molecular origin remains elusive, it is remarkable that three species emerge from the data. Under normal conditions in seawater, forces as large as those associated with the chair-to-boat transitions, i.e., >400 pN/strand, are rather unlikely; however, the observed transitions indicate that there is an extra extensibility in the marine gel should an extreme mechanical exposure arise.

At higher levels of fibril entanglement, we obtain force-extension curves that contain more complex patterns: sawtooth patterns, force plateaus, and force steps. The sawtooth patterns arise from the unraveling of globular polysaccharide entanglements. The force plateaus are attributed to the unzipping of intertwined fibrils (helices). These morphologies are able to withstand large forces (up to 400 pN), suggesting that lateral stability may be important in maintaining the structural integrity of the marine gel. Finally, force staircases arise from the peeling of fibrils from the junction zones in marine-gel networks. The number, step size, and length of the steps depend on the morphology of the gel and the strength of association of fibrils within. Indeed, swelling the gel by reducing the salinity of seawater leads to more extended, weaker structures. The striking similarity between the nanomechanical behavior of the marine gel and that of purified polysaccharide components indicates that their global structural and mechanical properties are defined by the polysaccharide component.

From a broader perspective, our approach can be used to design experiments to study mechanical properties of other complex biopolymer networks, such as the extracellular matrix in living tissues, microbial biofilms, or gel matrices, for a variety of technological applications.

SUPPORTING MATERIAL

Supporting Materials and Methods and three figures are available at http://www.biophysj.org/biophysj/supplemental/S0006-3495(14)00604-3.

The authors are particularly grateful to Ranieri Urbani for providing the purified polysaccharides isolated from the marine gels and *C. closterium* culture medium. V.S., M.K., and G.P. thank COST Action TD1002 for supporting their networking activities.

This work is supported by the Croatian Ministry of Science, Education and Sport (by the project Surface Forces on an Atomic Scale Applied in Marine Science and Nanotechnology No. 0982934-2744). Partial support was provided by the MRSEC Program of the National Science Foundation under grant no. DMR-0820341, National Science Foundation Career Grant no. 0955621, and grants from the Hungarian Science Foundation (OTKA K84133 and OTKA K109480). G.P.'s stay with the J.B. group at the Department of Physics, New York University, was financed through a Croatian Science Foundation Doctoral Fellowship Award.

SUPPORTING CITATIONS

References (62,63) appear in the Supporting Material.

REFERENCES

1. Verdugo, P., A. L. Alldredge, …, P. H. Santschi. 2004. The oceanic gel phase: a bridge in the DOM–POM continuum. *Mar. Chem.* 92:67–85.
2. Azam, F., and R. A. Long. 2001. Sea snow microcosms. *Nature.* 414:495–498, 497–498.
3. Žutić, V., and V. Svetličić. 2000. Interfacial processes. *In* The Handbook of Environmental Chemistry. P. Wangersky, editor. Springer-Verlag, Berlin, pp. 150–164.
4. Passow, U. 2002. Transparent exopolymer particles (TEP) in aquatic environments. *Prog. Oceanogr.* 55:287–333.
5. Verdugo, P. 2012. Marine microgels. *Annu. Rev. Mar. Sci.* 4:375–400.
6. Vollenweider, R. A., and A. Rinaldi, editors. 1995. Marine mucilages. *Sci. Total Environ.* 165 (special issue).
7. Giani, M., D. Degobbis, and A. Rinaldi, editors. 2005. Mucilages in the Adriatic and Tyrrhenian Seas. *Sci. Total Environ.* 353 (special issue).
8. Svetličić, V., V. Zutić, …, R. Urbani. 2011. Polymer networks produced by marine diatoms in the northern Adriatic sea. *Mar. Drugs.* 9:666–679.
9. Kepkay, P. E. 1994. Particle aggregation and the biological reactivity of colloids. *Mar. Ecol. Prog. Ser.* 109:293–304.
10. Azam, F. 1998. Microbial control of oceanic carbon flux: the plot thickens. *Science.* 280:694–696.
11. Kovač, N., P. Mozetić, …, C. Defarge. 2005. Phytoplankton composition and organic matter organization of mucous aggregates by means of light and cryo-scanning electron microscopy. *Mar. Biol.* 147:261–271.
12. Radić, T. M., V. Svetličić, …, B. Boulgaropoulos. 2011. Seawater at the nanoscale: marine gel imaged by atomic force microscopy. *J. Mol. Recognit.* 24:397–405.
13. Santschi, P. H., E. Balnois, …, J. Buffle. 1998. Fibrillar polysaccharides in marine macromolecular organic matter as imaged by atomic force microscopy and transmission electron microscopy. *Limnol. Oceanogr.* 43:896–908.
14. Aluwihare, L. I., and D. J. Repeta. 1999. A comparison of the chemical characteristics of oceanic DOM and extracellular DOM produced by marine algae. *Mar. Ecol. Prog. Ser.* 186:105–117.
15. McCarthy, M., J. Hedges, and R. Benner. 1996. Major biochemical composition of dissolved high molecular weight organic matter in seawater. *Mar. Chem.* 55:281–297.
16. Giani, M., D. Berto, …, R. Urbani. 2005. Chemical characterization of different typologies of mucilaginous aggregates in the Northern Adriatic Sea. *Sci. Total Environ.* 353:232–246.
17. Urbani, R., and A. Cesaro. 2001. Chain conformations of polysaccharides in different solvents. *In* Handbook of Solvents. G. Wypych, editor. ChemTec Publishing, Toronto, pp. 706–735.
18. Müller-Niklas, G., S. Schuster, …, G. J. Herndl. 1994. Organic content and bacterial metabolism in amorphous aggregations of the northern Adriatic Sea. *Limnol. Oceanogr.* 39:58–68.
19. Panagiotopoulos, C., and R. Sempéré. 2005. Analytical methods for the determination of sugars in aquatic environments: a historical perspective and future directions. *Limnol. Oceanogr. Methods.* 3:419–454.
20. Urbani, R., E. Magaletti, …, A. M. Cicero. 2005. Extracellular carbohydrates released by the marine diatoms *Cylindrotheca closterium, Thalassiosira pseudonana* and *Skeletonema costatum*: effect of P-depletion and growth status. *Sci. Total Environ.* 353:300–306.
21. Pletikapić, G., T. M. Radić, …, V. Zutić. 2011. AFM imaging of extracellular polymer release by marine diatom *Cylindrotheca closterium* (Ehrenberg) Reiman & J.C. Lewin. *J. Mol. Recognit.* 24:436–445.
22. Urbani, R., P. Sist, …, V. Žutić. 2012. Diatom polysaccharides: extracellular production, isolation and molecular characterization. *In* The Complex World of Polysaccharides. D. N. Karunaratn, editor. InTech, Rijeka, Croatia, pp. 345–370.
23. Rinaudo, M. 2005. Advances in characterization of polysaccharides in aqueous solution and gel state. *In* Polysaccharides-Structural Diversity and Functional Versatility. S. Dumitriu, editor. CRC Press, Boca Raton, FL, pp. 237–252.
24. Israelachvili, J. N. 2010. Intermolecular and Surface Forces. Academic Press, London.
25. Cesàro, A., B. Bellich, and M. Borgogna. 2012. Biophysical functionality in polysaccharides: from Lego-blocks to nano-particles. *Eur. Biophys. J.* 41:379–395.
26. Chin, W.-C., M. V. Orellana, and P. Verdugo. 1998. Spontaneous assembly of marine dissolved organic matter into polymer gels. *Nature.* 391:568–572.
27. Ding, Y.-X., W.-C. Chin, …, P. Verdugo. 2008. Amphiphilic exopolymers from *Sagittula stellata* induce DOM self-assembly and formation of marine microgels. *Mar. Chem.* 112:11–19.
28. Dogsa, I., M. Kriechbaum, …, P. Laggner. 2005. Structure of bacterial extracellular polymeric substances at different pH values as determined by SAXS. *Biophys. J.* 89:2711–2720.
29. Dammer, U., O. Popescu, …, G. N. Misevic. 1995. Binding strength between cell adhesion proteoglycans measured by atomic force microscopy. *Science.* 267:1173–1175.
30. Verdugo, P., and P. H. Santschi. 2010. Polymer dynamics of DOC networks and gel formation in seawater. *Deep Sea Res. Part II Top. Stud. Oceanogr.* 57:1486–1493.
31. Zoppini, A., A. Puddu, …, P. Sist. 2005. Extracellular enzyme activity and dynamics of bacterial community in mucilaginous aggregates of the Northern Adriatic Sea. *Sci. Total Environ.* 353:270–286.
32. Pletikapić, G., V. Žutić, …, V. Svetličić. 2012. Atomic force microscopy characterization of silver nanoparticles interactions with marine diatom cells and extracellular polymeric substance. *J. Mol. Recognit.* 25:309–317.
33. Svetličić, V., V. Zutić, …, T. M. Radić. 2013. Marine polysaccharide networks and diatoms at the nanometric scale. *Int. J. Mol. Sci.* 14:20064–20078.
34. Bustamante, C., J. F. Marko, …, S. Smith. 1994. Entropic elasticity of λ-phage DNA. *Science.* 265:1599–1600.
35. Bouchiat, C., M. D. Wang, …, V. Croquette. 1999. Estimating the persistence length of a worm-like chain molecule from force-extension measurements. *Biophys. J.* 76:409–413.
36. Kellermayer, M. S. Z., S. B. Smith, …, C. Bustamante. 1997. Folding-unfolding transitions in single titin molecules characterized with laser tweezers. *Science.* 276:1112–1116.
37. Camesano, T. A., and N. I. Abu-Lail. 2002. Heterogeneity in bacterial surface polysaccharides, probed on a single-molecule basis. *Biomacromolecules.* 3:661–667.
38. Higgins, M. J., P. Molino, …, R. Wetherbee. 2003. The structure and nanomechanical properties of the adhesive mucilage that mediates diatom-substratum adhesion and motility. *J. Phycol.* 39:1181–1193.
39. Rief, M., F. Oesterhelt, …, H. E. Gaub. 1997. Single molecule force spectroscopy on polysaccharides by atomic force microscopy. *Science.* 275:1295–1297.
40. Marszalek, P. E., A. F. Oberhauser, …, J. M. Fernandez. 1998. Polysaccharide elasticity governed by chair-boat transitions of the glucopyranose ring. *Nature.* 396:661–664.
41. Li, H., M. Rief, …, J. Shen. 1999. Single-molecule force spectroscopy on polysaccharides by AFM: nanomechanical fingerprint of α1,4-linked polysaccharides. *Chem. Phys. Lett.* 305:197–201.
42. Marszalek, P. E., H. Li, and J. M. Fernandez. 2001. Fingerprinting polysaccharides with single-molecule atomic force microscopy. *Nat. Biotechnol.* 19:258–262.
43. Cappiello, A., H. Trufelli, …, N. Penna. 2007. Study on the oligosaccharides composition of the water-soluble fraction of marine mucilage by electrospray tandem mass spectrometry. *Water Res.* 41:2911–2920.
44. Wolfgang, A. L., and A. Grützner. 2008. Pulling single molecules of titin by AFM—recent advances and physiological implications. *Pflugers Arch.* 456:101–115.

45. Carrion-Vazquez, M., H. Li, …, J. M. Fernandez. 2003. The mechanical stability of ubiquitin is linkage dependent. *Nat. Struct. Biol.* 10:738–743.

46. Dugdale, T. M., R. Dagastine, …, R. Wetherbee. 2006. Diatom adhesive mucilage contains distinct supramolecular assemblies of a single modular protein. *Biophys. J.* 90:2987–2993.

47. Dugdale, T. M., A. Willis, and R. Wetherbee. 2006. Adhesive modular proteins occur in the extracellular mucilage of the motile, pennate diatom *Phaeodactylum tricornutum*. *Biophys. J.* 90: L58–L60.

48. Zhang, W., and X. Zhang. 2003. Single molecule mechanochemistry of macromolecules. *Prog. Polym. Sci.* 28:1271–1295.

49. Xu, Q., S. Zou, …, X. Zhang. 2001. Single-molecule force spectroscopy on carrageenan by means of AFM. *Macromol. Rapid Commun.* 22:1163–1167.

50. Li, H., M. Rief, …, H. E. Gaub. 1998. Single-molecule force spectroscopy on xanthan by AFM. *Adv. Mater.* 10:316–319.

51. Li, H., M. Rief, …, H. E. Gaub. 1999. Force spectroscopy on single xanthan molecules. *Appl. Phys. A Mater. Sci. Process.* 68:407–410.

52. Zhang, L., C. Wang, …, X. Zhang. 2003. Single-molecule force spectroscopy on curdlan: unwinding helical structures and random coils. *Nano Lett.* 3:1119–1124.

53. Scherer, A., C. Zhou, …, A. Zumbusch. 2005. Intermolecular interactions of polymer molecules determined by single-molecule force spectroscopy. *Macromolecules.* 38:9821–9825.

54. Kellermayer, M. S., L. Grama, …, B. Penke. 2005. Reversible mechanical unzipping of amyloid β-fibrils. *J. Biol. Chem.* 280:8464–8470.

55. Karsai, A., Z. Mártonfalvi, …, M. S. Kellermayer. 2006. Mechanical manipulation of Alzheimer's amyloid β1–42 fibrils. *J. Struct. Biol.* 155:316–326.

56. Murvai, U., K. Soós, …, M. S. Kellermayer. 2011. Effect of the β-sheet-breaker peptide LPFFD on oriented network of amyloid β25–35 fibrils. *J. Mol. Recognit.* 24:453–460.

57. Chatellier, X., T. J. Senden, …, J. M. Di Meglio. 1998. Detachment of a single polyelectrolyte chain adsorbed on a charged surface. *Europhys. Lett.* 41:303–308.

58. Haupt, B. J., J. Ennis, and E. M. Sevick. 1999. The detachment of a polymer chain from a weakly adsorbing surface using an AFM tip. *Langmuir.* 15:3886–3892.

59. Conti, M., Y. Bustanji, …, B. Samorì. 2001. The desorption process of macromolecules adsorbed on interfaces: the force spectroscopy approach. *ChemPhysChem.* 2:610–613.

60. Hugel, T., M. Grosholz, …, M. Seitz. 2001. Elasticity of single polyelectrolyte chains and their desorption from solid supports studied by AFM based single molecule force spectroscopy. *Macromolecules.* 34:1039–1047.

61. Friedsam, C., A. D. C. Becares, …, H. E. Gaub. 2004. Adsorption of polyacrylic acid on self-assembled monolayers investigated by single-molecule force spectroscopy. *New J. Phys.* 6:1–16.

62. Balnois, E., and K. J. Wilkinson. 2002. Sample preparation techniques for the observation of environmental biopolymers by atomic force microscopy. *Colloids Surf. A Physicochem. Eng. Asp.* 207:229–242.

63. Rabbi, M., and P. Marszalek. 2007. Measuring polysaccharide mechanics by atomic force microscopy. *CSH Protoc.* 2007. http://dx.doi.org/10.1101/pdb.prot4900.